

## Review

# Neuropathological staging of Alzheimer-related changes

H. Braak and E. Braak\*

Zentrum der Morphologie, Theodor-Stern-Kai 7, W-6000 Frankfurt/Main 70, Federal Republic of Germany

Received March 6, 1991/Revised May 17, 1991/Accepted June 3, 1991

**Summary.** Eighty-three brains obtained at autopsy from nondemented and demented individuals were examined for extracellular amyloid deposits and intraneuronal neurofibrillary changes. The distribution pattern and packing density of amyloid deposits turned out to be of limited significance for differentiation of neuropathological stages. Neurofibrillary changes occurred in the form of neuritic plaques, neurofibrillary tangles and neuropil threads. The distribution of neuritic plaques varied widely not only within architectonic units but also from one individual to another. Neurofibrillary tangles and neuropil threads, in contrast, exhibited a characteristic distribution pattern permitting the differentiation of six stages. The first two stages were characterized by an either mild or severe alteration of the transentorhinal layer Pre- $\alpha$  (transentorhinal stages I–II). The two forms of limbic stages (stages III–IV) were marked by a conspicuous affection of layer Pre- $\alpha$  in both transentorhinal region and proper entorhinal cortex. In addition, there was mild involvement of the first Ammon's horn sector. The hallmark of the two isocortical stages (stages V–VI) was the destruction of virtually all isocortical association areas. The investigation showed that recognition of the six stages required qualitative evaluation of only a few key preparations.

**Key words:** Amyloid – Neurofibrillary changes – Dementia – Alzheimer's disease – Staging

The neuropathological hallmark of Alzheimer's disease (AD) is the progressive accumulation of insoluble fibrous material which is normally not found in the human central nervous system. This material consists of extracellular amyloid [15, 18, 19, 40, 43, 62] and intraneuronal neurofibrillary (NF) changes [4, 8, 39, 53, 55, 56, 59]. Furthermore, it is not distributed at random

but shows a characteristic pattern [3, 9, 10, 14, 31, 33, 34, 38, 48, 58].

End-stages of AD are easily recognized at neuropathological examination. Evaluation of cases with mild to moderate affection, in contrast, is fraught with difficulties. Currently, quantitative analyses of numerous areas are required for distinction of fully developed AD from cases with insufficiently dense changes [32, 35]. Little effort has as yet been made to further differentiate cases which do not meet the conventional diagnostic criteria [9]. Upon evaluation of a large number of cases with various degrees of involvement the existence of characteristic changes in the distribution pattern of neurofibrillary tangles (NFT) and neuropil threads (NT) became apparent (Tables 1, 2). It is tempting to assume that this sequence of involvement also reflects – in a still unknown manner – the clinical course of AD. This study, however, is not aimed at correlating morphological changes with clinical symptoms but tries to show differences in the pattern of NFT and NT rendering morphological staging of AD-related changes possible.

## Materials and methods

A total of 83 brains obtained at autopsy and fixed by immersion into a 4% aqueous solution of formaldehyde was used for this study. None of the brains had macroscopically detectable infarctions. Eight brains were from individuals whose clinical protocols included the diagnosis of dementia (Table 2, nos. 45, 47, 48, 52–54, 56, 59); however, at neuropathological examination these brains did not meet the conventional criteria for diagnosis of fully developed AD [9, 35]. Twenty-one brains were from demented old-aged individuals (nos. 62–83) including four brains from patients who had suffered from Down's syndrome (nos. 70, 71, 74, 75). Brains 62–83 displayed sufficient densities of isocortical NF changes [32, 35] to confirm the clinical diagnosis of AD.

The brains were cut into hemispheres. One hemisphere of each brain was then cut into blocks in the frontal plane with the aid of a macrotome. Fourty brains (marked in Table 2 by an asterisk) were cut into 12–14 blocks. Of the remaining 43 brains only 4 blocks (frontal, anterior central: uncus level, posterior central: CGL level, occipital) were used in the study. The blocks were embedded

\* Supported by the Deutsche Forschungsgemeinschaft

Offprint requests to: H. Braak (address see above)

**Table 1.** Stages in the gradual accumulation of neurofibrillary tangles (NFT) and neuropil threads (NT)

Location	Stage: I	II	III	IV	V	VI
Cortical areas:						
Fascia dentata	0	0	0	0	0-i	+--+
CA4: Non-pyramidal cells	0	0	0	i-+	+--+	+++g
CA4/CA3: Pyramidal cells	0	0	0	0	i-+	+--+
CA1: Pyramidal cells	0	i-+	+--+	++	+++	+++g
Subiculum	0	0	0	i	+	+--+
Presubiculum	0	0	0	0	0-i	+
Para-/Transsubiculum	0	0	0	0-i	+	++
Entorhinal-Pre- $\alpha$	0-i	+	++	+++	+++g	+++g
Entorhinal-Pri- $\alpha$	0	i	+	+--+	++	+++g
Entorhinal-Pre- $\beta$	0	0	i	+	+--+	++
Transentorhinal Pre- $\alpha$	i-+	+--+	++	+++g	+++g	+++g
Isocortex:						
Association areas	0	0	i	+	+++	+++
Parastriate area	0	0	0-i	i-+	+	++
Striate area	0	0	0	0-i	i-+	+
Subcortical nuclei:						
Striatum	0	0	i	i-+	+	++
Basal magnocellular complex	0	i	+	+--+	++	+++g
Amygdala	0	i	+	++	+++	+++g
Clastrum	0	0	0	i	+	++
Thalamus:						
Antero-dorsal nucleus	i	i-+	+--+	++	+++g	+++g
Reuniens nucleus	0	0	i	+	++	+++
Reticular nucleus	0	0	0	i	+	++
Hypothalamus:						
Tuberomamillary nucleus	0	0	i	+	++	+++
Lateral tuberal nucleus	0	0	0	0	i	+
Pars compacta of substantia nigra	0	0	0	0	i	+--+

The overall amount of NFT and NT is graded and labeled zero (0) with no discernible change, (i) with a few isolated NFT, or (+) with small, (++) moderate, and (+++) large numbers of NFT and NT. (g) points to the presence of ghost tangles

in polyethylene glycol (PEG 1000, Merck; [51]), sectioned at 100  $\mu$ m and stained for amyloid [17], NF changes [13, 25, 26] and in some instances for lipofuscin and basophilic material [2] (for details of the advanced silver techniques used for the detection of brain amyloid and NF changes see [6, 7, 11]). The distribution pattern of structures immunoreactive with antibodies against A4 amyloid protein or paired helical filaments mirrors the pattern seen after application of the respective silver techniques [7, 14, 16]. The silver technique for amyloid occasionally shows weak to intense co-staining of axons (Figs. 1a, d-f, 3; white matter, alveus, fornix). This nonspecific staining can easily be distinguished from amyloid.

Additional blocks from the other hemisphere were paraffin embedded, sectioned at 12  $\mu$ m and stained with cresyl violet, congo red, conventional silver techniques (Bodian, Bielschowsky), and the above-mentioned methods (Campbell-Switzer, Gallyas). Paraffin sections were also immunostained for A4 amyloid protein and NF changes. Differentiation of neuropathological stages can also be carried out in paraffin sections. Due to the fact that many pathological structures superimpose each other in 100- $\mu$ m-thick sections the distribution pattern of the pathological material is more clearly displayed in polyethylene glycol preparations [11, 15].

## Results

The brains examined in this study either remain devoid of AD-related changes or display varying amounts of amyloid deposits and/or NF changes (Table 2).

### Amyloid deposits

The cerebral cortex, in particular the isocortex, is the predilection site for the deposition of amyloid (Fig. 1). The forebrains of quite a number of old-aged individuals remain devoid of such deposits, while those of demented individuals harbor large amounts of amyloid.

The plaque-like deposits show considerable variations in shape and size. Most of them remain devoid of pathologically changed argyrophilic nerve cells processes and show neither distortions of the neuropil nor accumulations of glial cells. The nerve cells situated within the deposits appear virtually unchanged (see also [41]). Amyloid deposits, therefore, should not be confused with "neuritic" plaques [15].

Cases with severe NF changes consistently show high densities of amyloid deposits, while those rich in amyloid do not always turn out to be affected by NF changes (Table 2). A few cases with moderate NF changes do not reveal the presence of amyloid (stage I: 4 out of 13 cases, stage II: 7 out of 17 cases, stage III: 1 out of 10 cases; Table 2).

The end-stage of amyloid accumulation is characterized by a fairly constant distribution pattern of the pathological material. In contrast, early stages exhibit considerable inter-individual variation, thus, rendering the differentiation of only three stages possible.

**Table 2.** Sex, age, and neuropathological stage of accumulation of both amyloid deposits (A–C) and neurofibrillary (NF) changes (I–VI)

No.	Sex	Age	Clinically proven dementia	Amyloid deposits	NF changes	Deviation from pattern displayed in Table 1
1*	f	47		A	0	
2*	m	56		B	0	
3*	f	58		B	0	
4	m	60		0	0	
5*	f	65		0	0	
6	f	67		A	0	
7	f	67		0	0	
8*	f	81		A	0	
9	f	85		B	0	
10	m	85		0	0	
11*	f	96		A	0	
Mean:		67				
12	f	54		0	I	
13	m	60		0	I	
14*	m	62		A	I	
15	m	63		A	I	
16*	m	67		B	I	
17*	m	71		A	I	
18*	f	74		A	I	
19*	f	75		A	I	
20	m	82		B	I	
21*	f	83		0	I	
22*	m	84		0	I	
23*	m	84		A	I	
24*	f	94		A	I	
Mean:		74				
25	f	47		0	II	CA1 (-)
26	f	57		0	II	
27	m	58		A	II	
28	m	59		B	II	CA1 (-)
29	m	61		0	II	
30	m	65		0	II	
31	m	65		B	II	
32	f	66		B	II	
33*	f	72		B	II	CA1 (+)
34*	m	77		A	II	
35	f	77		A	II	trans e (+)
36	m	78		0	II	
37	m	79		0	II	
38	f	81		B	II	
39*	f	82		A	II	CA4 np (+)
40	f	84		B	II	
41	m	91		0	II	
Mean:		72				
42	m	58		B	III	CA1 (-)
43	m	71		A	III	
44*	f	75		A	III	
45*	m	76	D	B	III	
46*	m	78		C	III	CA4 np (+), parasub (+)
47*	m	79	D	B	III	
48*	f	82	D	C	III	CA1 (-)
49	m	83	D	B	III	CA1 (-)
50	f	84		0	III	
51	f	96	D	B	III	
Mean:		78.5				

**Table 2.** (continued)

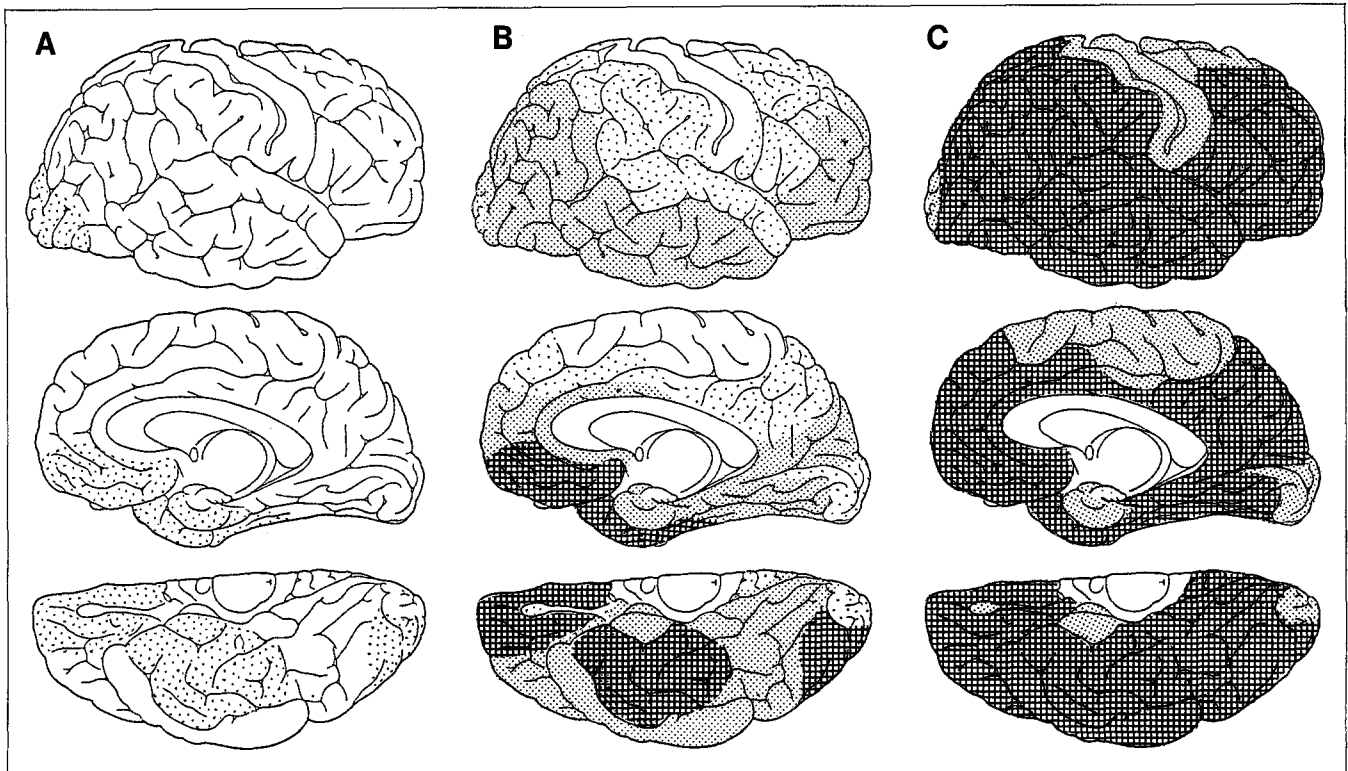
No.	Sex	Age	Clinically proven dementia	Amyloid deposits	NF changes	Deviation from pattern displayed in Table 1
52*	m	64	D	B	IV	CA1 (-)
53*	f	71	D	C	IV	
54*	f	71	D	C	IV	CA4 np (+)
55	f	73		B	IV	CA1 (+), e-Pri- $\alpha$ (+)
56*	m	78	D	C	IV	
57	f	78		C	IV	CA1 (+)
58*	f	85		A	IV	
59	m	83		C	IV	Parasub (-)
60	f	86	D	C	IV	Parasub (-)
61	m	90		C	IV	Parasub (-)
Mean:		78				
62*	m	77	D	C	V	
63	m	78	D	C	V	Sub (+)
64	f	80	D	C	V	Parasub (+)
65	m	81	D	C	V	CA4 np (+)
66	f	81	D	C	V	CA4 np (+), sub (+)
67*	f	81	D	C	V	
68*	f	81	D	C	V	Parasub (+), sub (+)
69*	m	89	D	C	V	Parasub (+), sub (+)
Mean:		81				
70	m	47	D	C	VI	
71*	f	56	D	C	VI	Parasub (+)
72	f	59	D	C	VI	
73	f	59	D	C	VI	
74	f	60	D	C	VI	
75	m	62	D	C	VI	
76	f	64	D	C	VI	
77*	m	64	D	C	VI	
78*	f	69	D	C	VI	Parasub (-)
79*	f	69	D	C	VI	Fd (-)
80*	f	71	D	C	VI	
81*	m	84	D	C	VI	
82*	f	87	D	C	VI	Presub (-)
83*	f	90	D	C	VI	Fd (-), CA4 np (-)
Mean:		64				

Graded series of sections running through an entire hemisphere were evaluated in cases marked by an asterisk. Cases with clinically proven dementia are indicated by "D". Deviations of the cortical involvement displayed in Table 1 are noted with (+) a step more-, or (-) a step less-intensive changes. f: female; m: male; CA1: first sector of the Ammon's horn; CA4 np: non pyramidal cells in the fourth sector of the Ammon's horn; e-Pri- $\alpha$ : entorhinal layer Pri- $\alpha$ ; Fd: fascia dentata; Parasub: parasubiculum; Presub: presubiculum; trans e: transentorhinal region; Sub: subiculum

*Stage A.* Low densities of amyloid deposits are first encountered in the isocortex and there particularly in the basal portions of the frontal, temporal, and occipital lobe (Figs. 1, 2a). The hippocampal formation remains devoid of amyloid. The parvocellular layer of the presubiculum and the entorhinal layers Pre- $\beta$  and Pre- $\gamma$  show weakly stained clouds or bands of amyloid frequently with ill-defined boundaries.

*Stage B.* Medium densities of amyloid deposits are present in almost all isocortical association areas at this stage. Only the primary sensory areas and the primary motor field remain free of deposits or contain only small amounts (Figs. 1, 2c). The belt areas and relatively large proportions of the frontal and parietal lobe adjoining the central region show scattered amyloid deposits (Fig. 1).

Typical laminar distribution is only found in the basal portions of the frontal, temporal and occipital isocortex (Fig. 2b). The external glial layer remains devoid of amyloid, while subjacent portions of layer I generally contain numerous patches which often show the tendency of blending into each other [14]. Layers II and III harbor relatively few globular deposits often marked by a condensed core. The myelin-rich layers IV and Vb (outer and inner line of Baillarger) contain weakly stained areas with ill-defined boundaries varying in size and shape. Layers Va and VI show intensely stained globular deposits decreasing in number from top to bottom. Frequently amyloid is also found in the white matter underlying the cortex. These deposits appear as agglomerations of small, condensed and intensely argyrophilic structures [14].



## Amyloid

**Fig. 1.** Distribution pattern of amyloid deposits. **Stage A** Initial deposits can be found in basal portions of the isocortex. **Stage B** The next stage shows amyloid in virtually all isocortical association areas. The hippocampal formation is only mildly involved. **Stage C**

In the end-stage deposits can be seen in all areas of the isocortex including sensory and motor core fields. Increasing density of shading indicates increasing numbers of amyloid deposits

The hippocampal formation is only mildly involved. Besides a few globular deposits restricted to the pyramidal layers of the subiculum and sector CA1, there are two conspicuous rows of small and densely packed deposits. One of these is located in the molecular layer of the subiculum gradually diminishing in width and density as it heads upwards into the upper half of stratum radiatum of CA1. The second row is confined to a narrow zone in the middle third of the molecular layer of the fascia dentata (Fig. 3). Sectors CA2 to CA4 contain only a few deposits. There is also some fluffy material deposited close to the free surface of the dentate gyrus (Fig. 3, arrow). A few cases show islands or bands of amyloid in both the superficial and profound pyramidal layer of CA1. The parvocellular layer of the presubiculum is filled with diffusely distributed amyloid [33]. Bands of amyloid may also be present in the entorhinal cortex.

*Stage C.* In stage C, virtually all isocortical areas (including the belt fields and primary areas) reveal densely packed deposits which basically remain arranged in their laminar distribution as described above (Fig. 2d-f). The hippocampal formation harbors relatively few deposits and shows the same pattern as

described for stage B (Fig. 3). Stage C, therefore, is mainly characterized by depositions of amyloid in primary isocortical areas [14]. Outside the cerebral cortex this stage shows gradual involvement of numerous subcortical structures. The striatum may become filled with amyloid [7]. A slightly less severe deposition of amyloid is seen in almost all nuclei of the thalamus and hypothalamus [10]. The subthalamic and red nucleus also show deposits, while the substantia nigra, pars compacta, remains virtually devoid of them. The molecular layer of the cerebellar cortex may exhibit many patches of amyloid [16].

### *Neurofibrillary changes*

Quite a number of the examined cases remain devoid of NF changes (Table 2, nos. 1-11). Demented individuals are severely affected and show large numbers of cortical and subcortical NF changes.

Three kinds of lesions can be distinguished, i.e., neuritic plaques, NFT and NT. Neuritic plaques (NP) are marked by a dense feltwork of argyrophilic nerve cell processes. In addition, diffuse amyloid deposits and/or amyloid cores are frequently present within the reaches

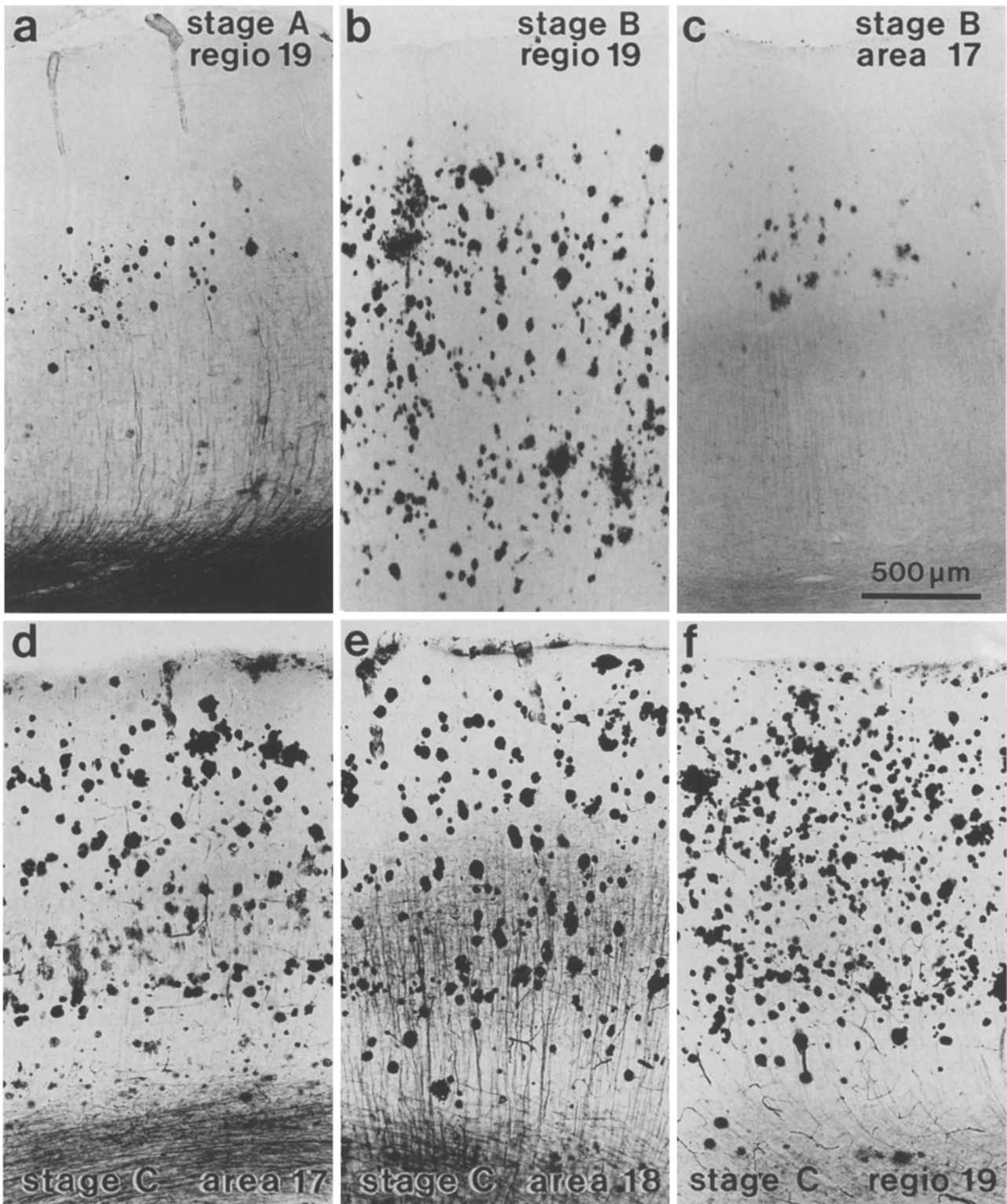


**Fig. 2.a-f.** Amyloid deposits in the occipital isocortex (layers I to VI). **a** Stage A displays a few patches of amyloid at mid-cortical level (basal occipital association cortex; case no. 39). **b,c** Stage B exhibits many amyloid deposits in virtually all association areas of the isocortex and occasionally a few dots in primary areas [**b** peristriate association cortex, **c** primary visual field (= area 17);

case no. 33]. **d-f** Stage C shows an abundance of amyloid in not only the association cortex but also in belt areas and core fields [**d** striate area (core, area 17), **e** parastriate area (belt, area 18), **f** peristriate region (association cortex, regio 19); case no. 76]. Scale in **c** is also valid for **a,b** and **d-f**. PEG sections, 100 µm, Campbell-Switzer

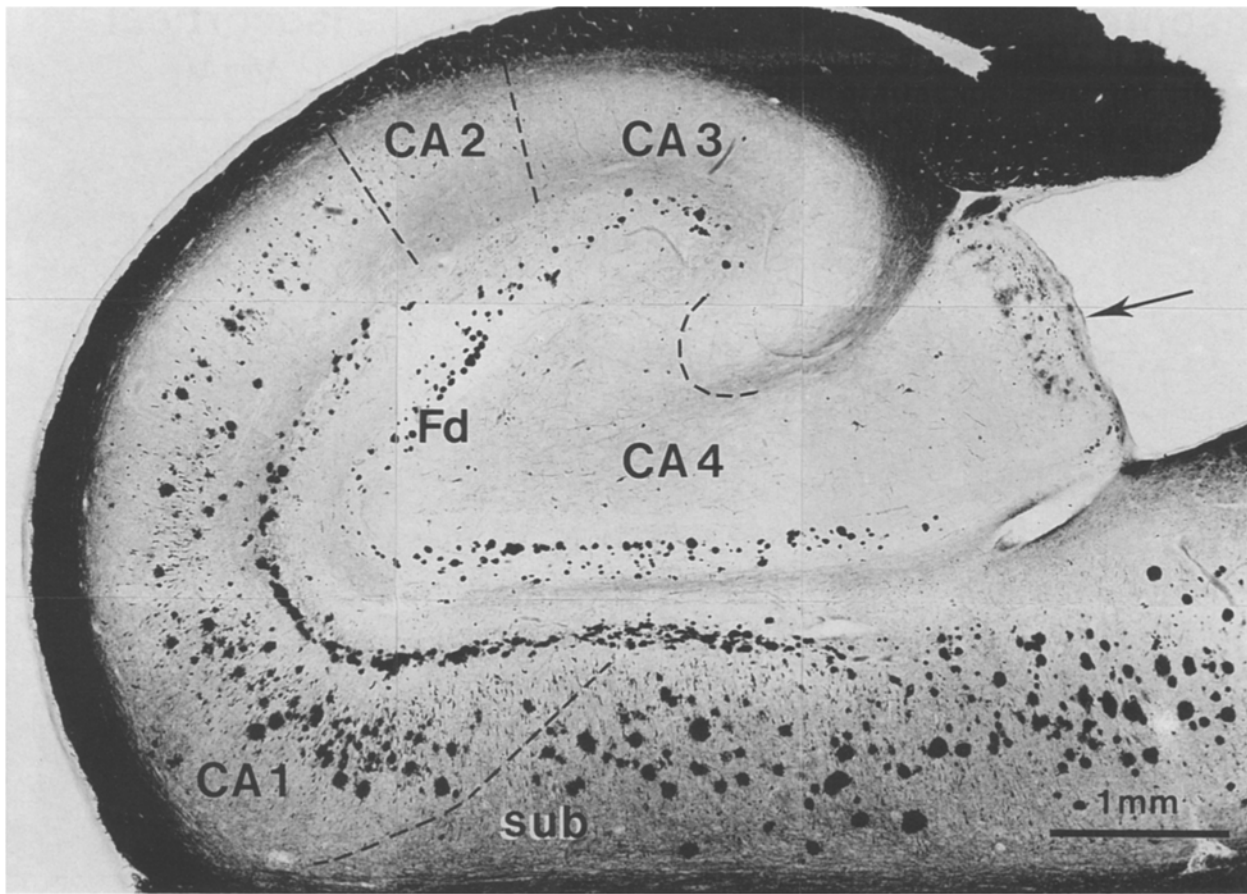


**Fig. 3.** Pattern of amyloid deposits in the hippocampal formation in stage C. Dotted lines indicate the boundaries of the subiculum (*sub*) and sectors CA1 to CA4. The arrow points to fluffy material accumulated along the free surface of the dentate gyrus. Note two rows of small and densely packed amyloid deposits. One is located

in the molecular layer of subiculum and upper half of stratum radiatum of CA1, the other appears in the molecular layer of the fascia dentata (*Fd*). Case no. 64; PEG section, 100  $\mu$ m, Campbell-Switzer

of such plaques [15]. Cortical territories covering the depth of the sulci generally show a larger number of NP than those located at the crest of the gyri [14, 28, 49, 59]. NFT develop within the nerve cell soma from where they may extend into the dendrites. The proximal axon remains free of such changes. Initial stages of NFT are located in the vicinity of lipofuscin deposits. After deterioration of the parent cell the NFT converts into an extraneuronal structure ("ghost tangle") eventually becoming engulfed and degraded by astrocytes. NT consist of argyrophilic processes of nerve cells loosely scattered throughout the neuropil. In the isocortex, they frequently occur in dendrites of tangle-bearing pyramidal cells. NT contribute considerably to the total NF changes [5, 9, 10, 12, 14, 63].

NFT and NT generally show a common and highly characteristic pattern of distribution with only minor inter-individual variations (Tables 1, 2). NP, in contrast, are much more irregularly distributed and, therefore, do not represent a useful tool for the differentiation of stages. Mainly because of the constancy of the pattern revealed by NFT and NT the distinction of the following stages is rendered possible (Tables, 1, 2, Fig. 4).

*Stage I.* The most mildly affected cases show an involvement of the cortex confined to the transentorhinal region. This is a complex transition zone located between the proper entorhinal region and the adjoining temporal isocortex. The distinguishing feature of this region is the superficial entorhinal cellular layer (Pre- $\alpha$ ) that follows an oblique course through the outer cortical layers. During this course the star-shaped Pre- $\alpha$  neurons gradually transform into pyramidal cells [2, 3, 9].

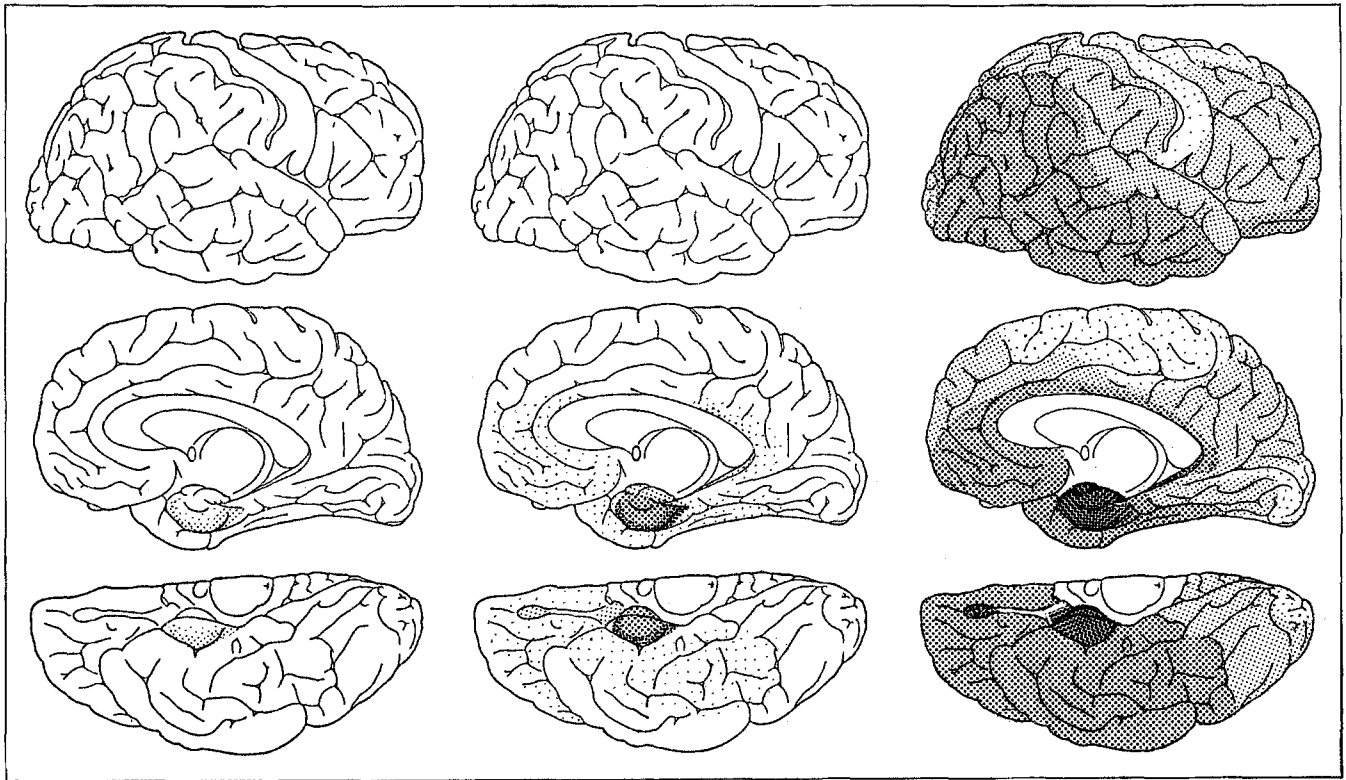
The transentorhinal Pre- $\alpha$  projection neurons generally are the first nerve cells in the brain to develop NFT and NT. Stage I is characterized by a modest number of these changes (Fig. 5a, and see Fig. 9, first row). A few isolated NFT may additionally occur in the proper entorhinal layer Pre- $\alpha$ , in sector CA1, in the magnocellular nuclei of the basal forebrain, and in the anterodorsal nucleus of the thalamus.

*Stage II.* The next stage is an aggravation of stage I and exhibits numerous NFT and NT in the transentorhinal Pre- $\alpha$  (Fig. 5b, note NT in the neighborhood of NFT). Their density decreases slightly when approaching the proper entorhinal Pre- $\alpha$ . The hippocampal sector CA1

**transentorhinal**  
**I - II**

**limbic**  
**III - IV**

**isocortical**  
**V - VI**



## Neurofibrillary changes

**Fig. 4.** Distribution pattern of neurofibrillary (NF) changes [neurofibrillary tangles (NFT) and neuropil threads (NT)]. Six stages (I-VI) can be distinguished. Stages I-II show alterations which are virtually confined to a single layer of the transentorhinal region (transentorhinal I-II). The key characteristic of stages III-IV is the

severe involvement of the entorhinal and transentorhinal layer Pre- $\alpha$  (limbic III-IV). Stages V-VI are marked by isocortical destruction (isocortical V-VI). Increasing density of shading indicates increasing severity of NF changes

and in particular its wedge-shaped extremity superimposing the subiculum is affected by modest numbers of NFT (see Fig. 8, third row, and Fig. 9, second row). The magnocellular forebrain nuclei and the antero-dorsal nucleus of the thalamus remain spared or show only mild changes. A few isolated NFT may inconstantly be encountered in isocortical association areas.

Stages I and II are characterized by the transentorhinal region being preferentially affected with only mild involvement of the hippocampus (CA1) and virtual absence of isocortical changes (Figs. 4, 9). They are, therefore, referred to as the "transentorhinal stages".

*Stage III.* The characteristic feature of the third stage is a severe involvement of layer Pre- $\alpha$ , both in the transentorhinal and entorhinal region. Many of the projection neurons within Pre- $\alpha$  contain a NFT. Numerous dendrites of these cells harbor NT, frequently rendering recognition of the extent of the dendritic tree possible. For the first time the presence of "ghost tangles" can be

observed in the transentorhinal layer Pre- $\alpha$ . A few NFT are also encountered in layers Pri- $\alpha$  and Pre- $\beta$  (Figs. 6a, 7, and Fig. 9, third row).

The hippocampal formation shows an only modest involvement of CA1 (Fig. 7, Fig. 8, third row, and Fig. 9, third row). Pyramidal cells of the subiculum start to develop NFT with particularly far-reaching extensions into the apical dendrite (Fig. 8o-q, and fourth row). Sectors CA2 to CA4 generally remain devoid of changes except of a few large multipolar nerve cells located close by or within the plexiform layer of the fascia dentata. These cells develop coarse NFT with far-reaching extension into the dendrites (Fig. 8c, d).

The isocortex remains virtually devoid of changes or is only mildly affected. Some individuals exhibit the presence of a few scattered NFT and NT within layers III and V in basal portions of frontal, temporal and occipital association areas. Others merely reveal a few irregularly distributed NP in layer III (Fig. 9, third row, and see Fig. 12).

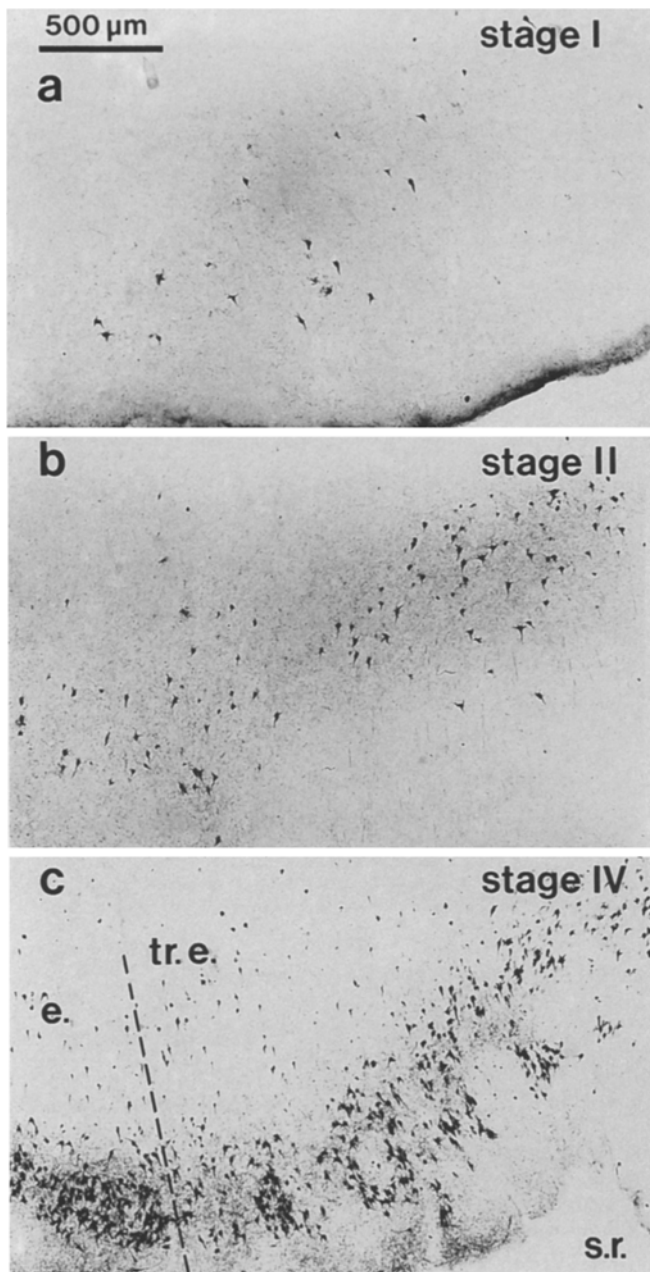


**Fig. 5a–c.** NFT and NT in the transentorhinal region. **a** A few scattered NFT can be seen in stage I (case no. 16). **b** The descent of layer Pre- $\alpha$  can be recognized in stage II (case no. 31). **c** The next two stages show a severe involvement of layer Pre- $\alpha$ . Note the dense accumulations of NT which are often found above the islands of NFT-bearing nerve cells. A dotted line shows the border between the entorhinal region and transentorhinal region (stage IV, case no. 52). Scale in **a** is also valid for **b–c**; *e.*: entorhinal region; *s.r.*: rhinal sulcus; *tr.e.*: transentorhinal region. PEG sections, 100  $\mu$ m, Gallyas

Most cases at this stage display mild changes of magnocellular forebrain nuclei, anterodorsal nucleus of the thalamus, and amygdala. Some isolated NFT may also occur in the reuniens nucleus of the thalamus and in the hypothalamic tuberomammillary nucleus.

*Stage IV.* The fourth stage is featured by the layer Pre- $\alpha$  being very severely affected (Figs. 5c, 6b). Large numbers of ghost tangles are present in both the transentorhinal and entorhinal region. There is also a considerable involvement of layers Pri- $\alpha$  and Pre- $\beta$  (Fig. 6b and Fig. 10, first row).

The hippocampal formation contains numerous NFT in CA1. The subiculum is only mildly involved (Fig. 8, fourth row). In addition, there is a modest affection with star-shaped tangles of the large multipolar CA4-nerve cells close to the fascia dentata (Fig. 8c,d, and second row).

The isocortex remains only mildly affected. Primary sensory areas and the primary motor field do not show changes or harbor only a few NP in layer III (Fig. 10, first row, and Figs. 11a, 12).

The corticomedial complex of the amygdala reveals the presence of many NP, while NFT and NT predominate in the basolateral nuclei. Basal portions of the claustrum are mildly affected. NFT may also appear in large neurons located in basal portions of the putamen and the accumbens nucleus. The reuniens nucleus and the tuberomammillary nucleus are slightly more intensely affected. The antero-dorsal thalamic nucleus is densely filled with NFT and NT (Fig. 13).

The key feature of stages III and IV is that both the entorhinal and transentorhinal layer Pre- $\alpha$  are conspicuously affected and that this is supplemented by a mild to moderate hippocampal and a still-low isocortical involvement (Figs. 4, 5c, 6a,b, 7, 11, 12). They are, therefore, summarized as “limbic stages”.

*Stage V.* Stage V shows severe changes with very large numbers of ghost tangles in layer Pre- $\alpha$ . The deep layer Pri- $\alpha$  is severely involved and appears as a band-like structure due to the large number of NT. In addition layers Pre- $\beta$  and even Pre- $\gamma$  are also distinctly affected (Fig. 6c and Fig. 10, second row). The parvocellular layers of both parasubiculum and transsubiculum show the presence of small NFT and numerous NT [33].

Virtually all components of the hippocampal formation are involved. Tangles within subicular pyramidal cells have far-reaching extensions into the apical dendrite (Fig. 8o–q, and fourth row) and can, therefore, easily be distinguished from the flame-shaped type of tangle seen in CA1 pyramidal neurons (Fig. 8k–n, and third row). A circumscribed portion of the uncus is marked by the presence of NFT with long extensions indicating a contribution of the anterior extremity of the subiculum to the formation of the uncus [2]. The development of particularly large numbers of NT is a further feature of the subicular pyramidal cell layer. NP occur predominantly in the wedge-shaped portion of CA1 abutting upon the subiculum. They are also found in lower numbers in the pyramidal cell layers of upper portions of CA1 (Fig. 8, third row), in CA2 and CA3. Sector CA1 is infested with NFT-bearing pyramidal cells. The outer pyramidal cell layer is more heavily involved than the inner one. In contrast, NFT are only occasionally observed in the stratum oriens. Besides the sparse network of NT seen throughout the pyramidal cell

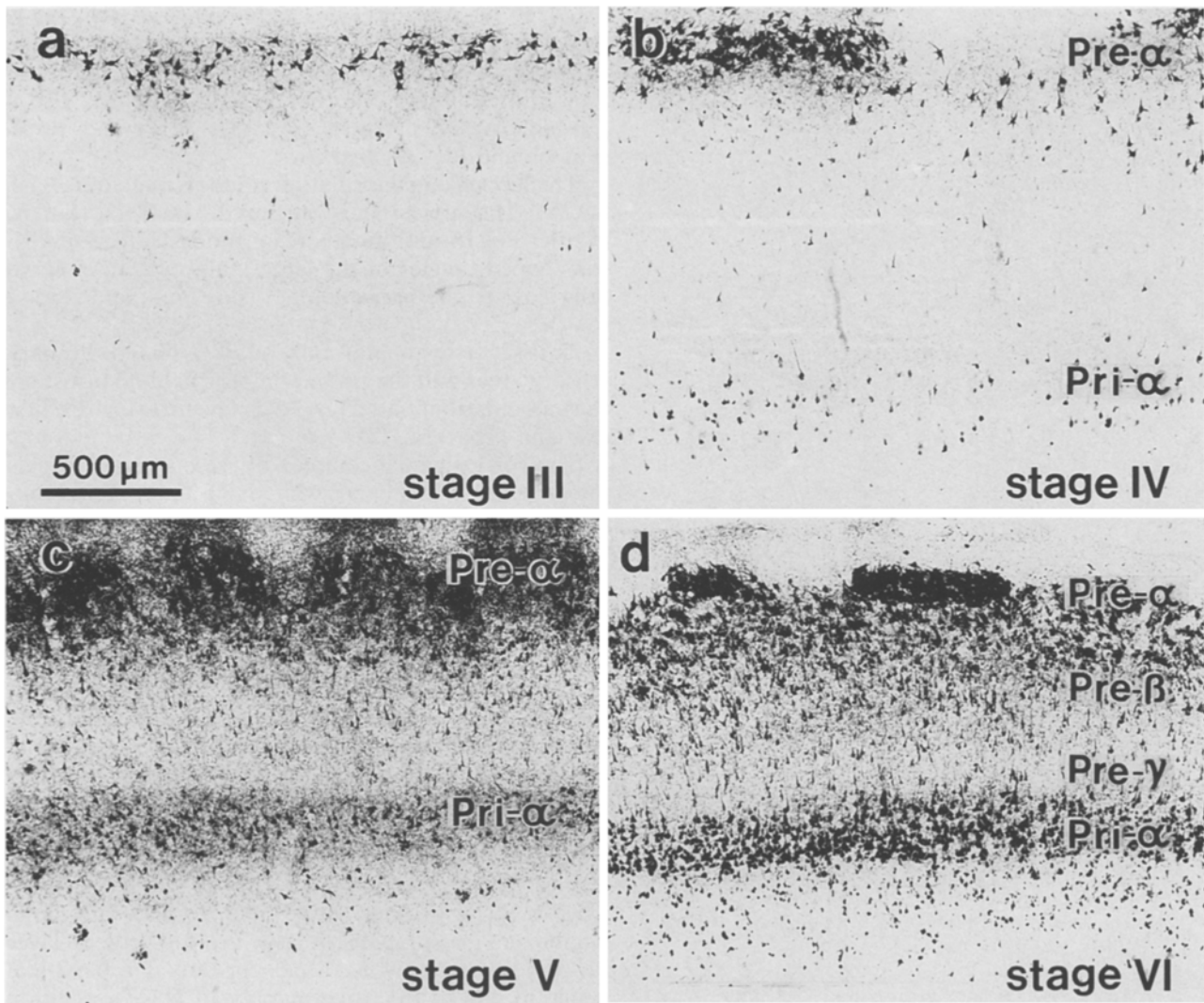
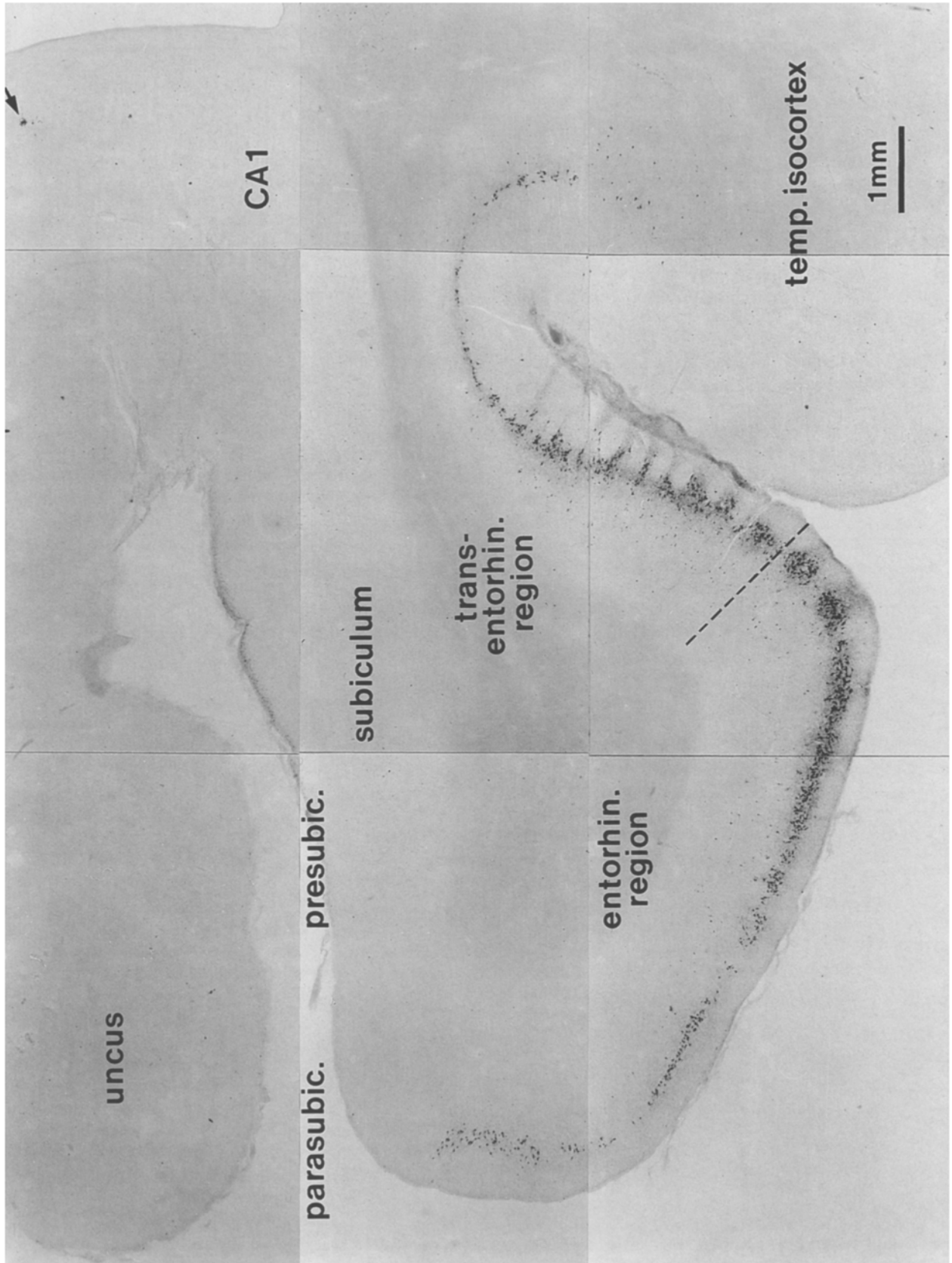


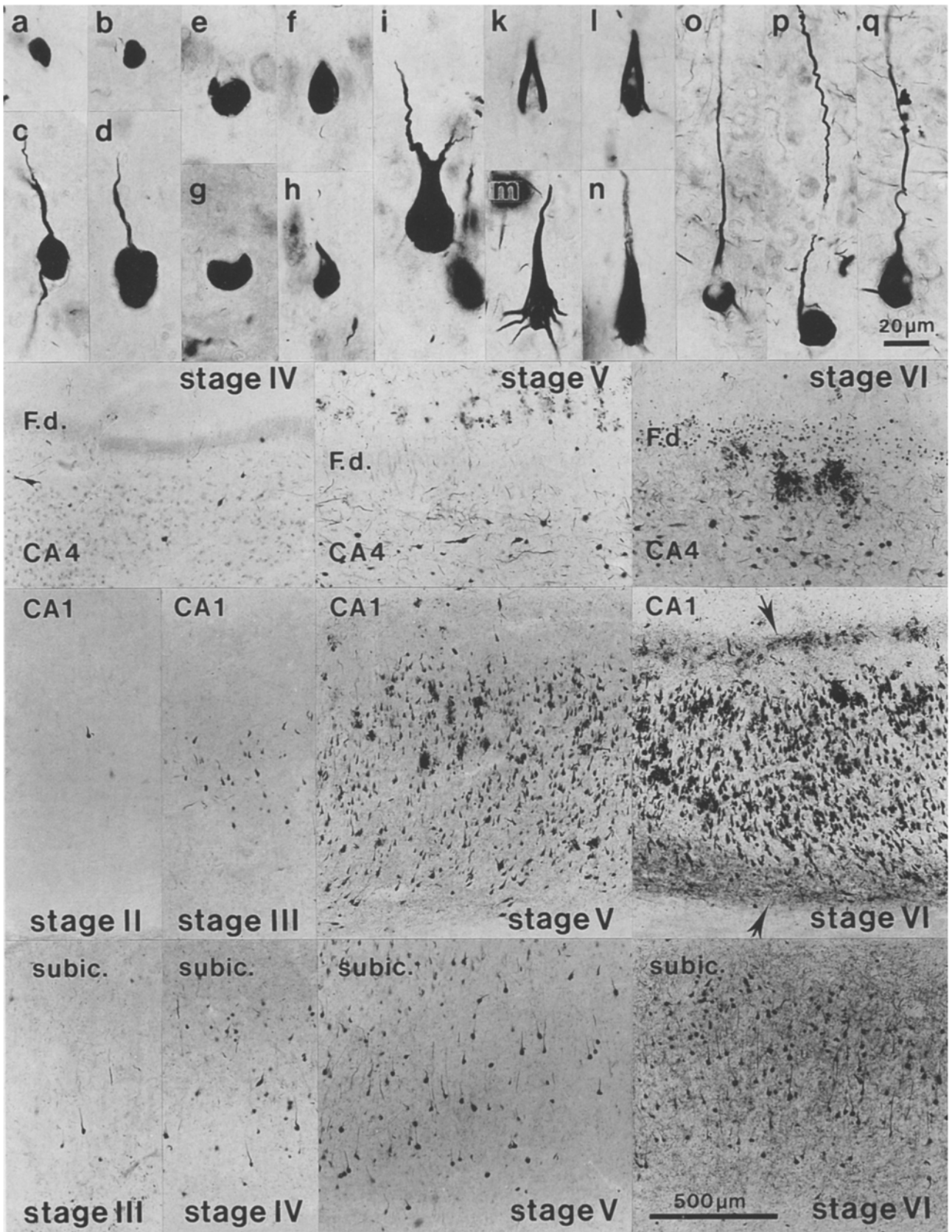
**Fig. 6a-d.** NFT and NT in the entorhinal region. **a** The characteristic islands of layer Pre- $\alpha$  are almost exclusively affected in stage III (case no. 48). **b** Mild involvement of the deep layer Pri- $\alpha$  is an additional feature of stage IV (case no. 52). **c** Severe destruction of Pre- $\alpha$  with a dense network of NT, marked involvement of Pri- $\alpha$  and even Pre- $\beta$  is encountered in stage V (case no. 67). **d** Even the end-stage VI reveals a gradation of involvement ranging from mild

changes in Pre- $\gamma$  to modest changes in Pre- $\beta$ , severe changes in Pri- $\alpha$  and very severe changes in Pre- $\alpha$  (case no. 79). With increasing density of NFT and NT there is also a decrease in the overall thickness of the cortex (compare the distance between layer Pre- $\alpha$  and Pri- $\alpha$  in stage IV with that in stage VI). Scale in **a** is also valid for **b-d**. PEG sections, 100  $\mu$ m, Gallyas

layers, two dense stripes of NT become visible, one accompanying the row of amyloid deposits and NP in the outer half of the stratum radiatum of CA1, the other outlining the stratum oriens (Fig. 8, third row). NF changes within sector CA2 are subject to considerable inter-individual variation. Frequently, the sector resists the development of changes but there are also cases with early and severe involvement of CA2. NFT in CA2 are coarse and generate stout extensions into both apical and basal dendrites (Fig. 8i). They, therefore, can readily be differentiated from NFT of CA1 and CA3 pyramidal cells. A few compact NFT occur within CA3 pyramidal cells and the modified pyramidal cells of CA4 [2] (Fig. 8e-h). NFT located within these cells remain confined

**Fig. 7.** Stage III is marked by conspicuous involvement of the transentorhinal and entorhinal layer Pre- $\alpha$  (case no. 48). This section runs through the uncus portion of the hippocampal formation. There is only very mild involvement of the first Ammon's horn sector [a single neuritic plaque (NP) is seen in the pyramidal layer of CA1, *arrow*]. The subiculum, pre- and parasubiculum remain unaffected. Similarly, the isocortex – in particular the adjoining temporal isocortex – is devoid of NF changes. Accordingly, this case does not show any involvement in the conventional section of the hippocampus cut at the level of the lateral geniculate body. CA1: First sector of the Ammon's horn; *entorhin.*: entorhinal; *parasubic.*: parasubiculum; *presubic.*: presubiculum; *temp.*: temporal, *transentorhin.*: transentorhinal; *dotted line*: border between entorhinal and transentorhinal region. PEG section, 100  $\mu$ m, Gallyas





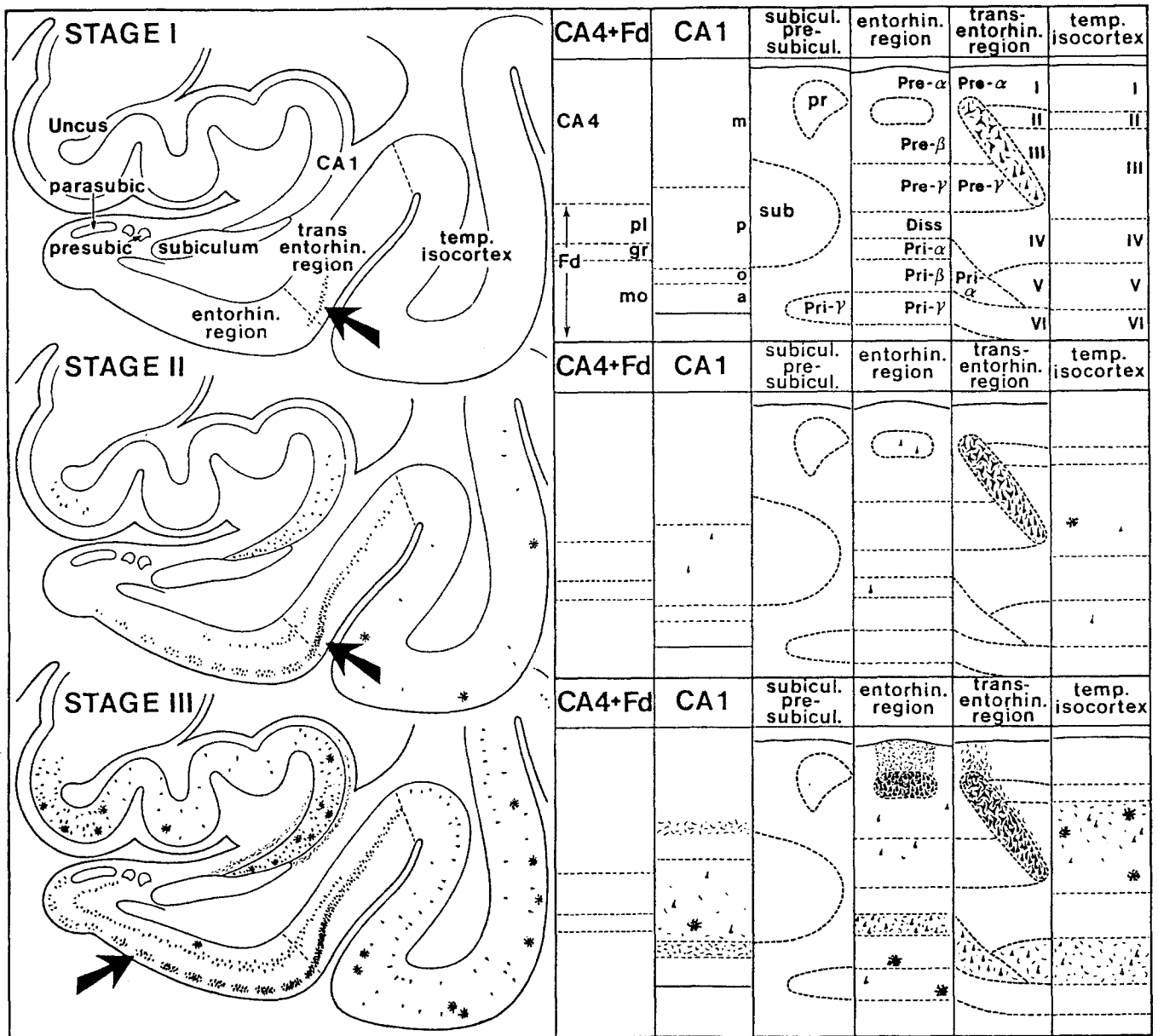


Fig. 9. (for legend see next page)

**Fig. 8.** NF changes in the hippocampal formation. *First row:* Various types of NFT as seen in different neuronal types of the hippocampal formation. Scale in **q** is also valid for **a-p**. **a,b** Globose NFT in granule cells of the fascia dentata. **c,d** NFT with extensions into dendrites of non-pyramidal neurons in the plexiform layer of the fascia dentata and adjoining portions of CA4. **e,f** Compact NFT in modified pyramidal cells of CA4. **g,h** The same type of NFT in pyramidal cells of CA3. **i** Large NFT in a CA2 pyramidal cell. **k-n** Flame-shaped NFT in superficial and deep pyramidal cells of CA1. **o-q** Slender tangles of the subiculum with long extensions into apical dendrites. *Second row:* NF changes in the fascia dentata (Fd.) and CA4. A few tangles located in non-pyramidal cells can be seen in stage IV (case no. 57). Their number increases considerably (stage V, case no. 66). The presence of many globose NFT in

granule cells of the fascia dentata is a distinguishing characteristic of stage VI (case no. 81). *Third row:* NF changes in the first sector of the Ammon's horn. Stages II-VI display increasing numbers of NFT. Note the dense lines of NT in the upper half of the stratum radiatum and in the stratum oriens indicated by arrows (stage II: case no. 32, stage III: case no. 50, stage V: case no. 68, stage VI: case no. 79). *Fourth row:* NF changes in the subiculum (subic.). In comparison to CA1 the subiculum shows presence of smaller numbers of NFT and a denser network of NT within its pyramidal cell layers (stage III: case no. 46, stage IV: case no. 61, stage V: case no. 68, stage VI: case no. 81). Scale shown in subiculum, stage VI, is also valid for all other micrographs in the second, third and fourth row. PEG sections, 100  $\mu$ m, Gallyas

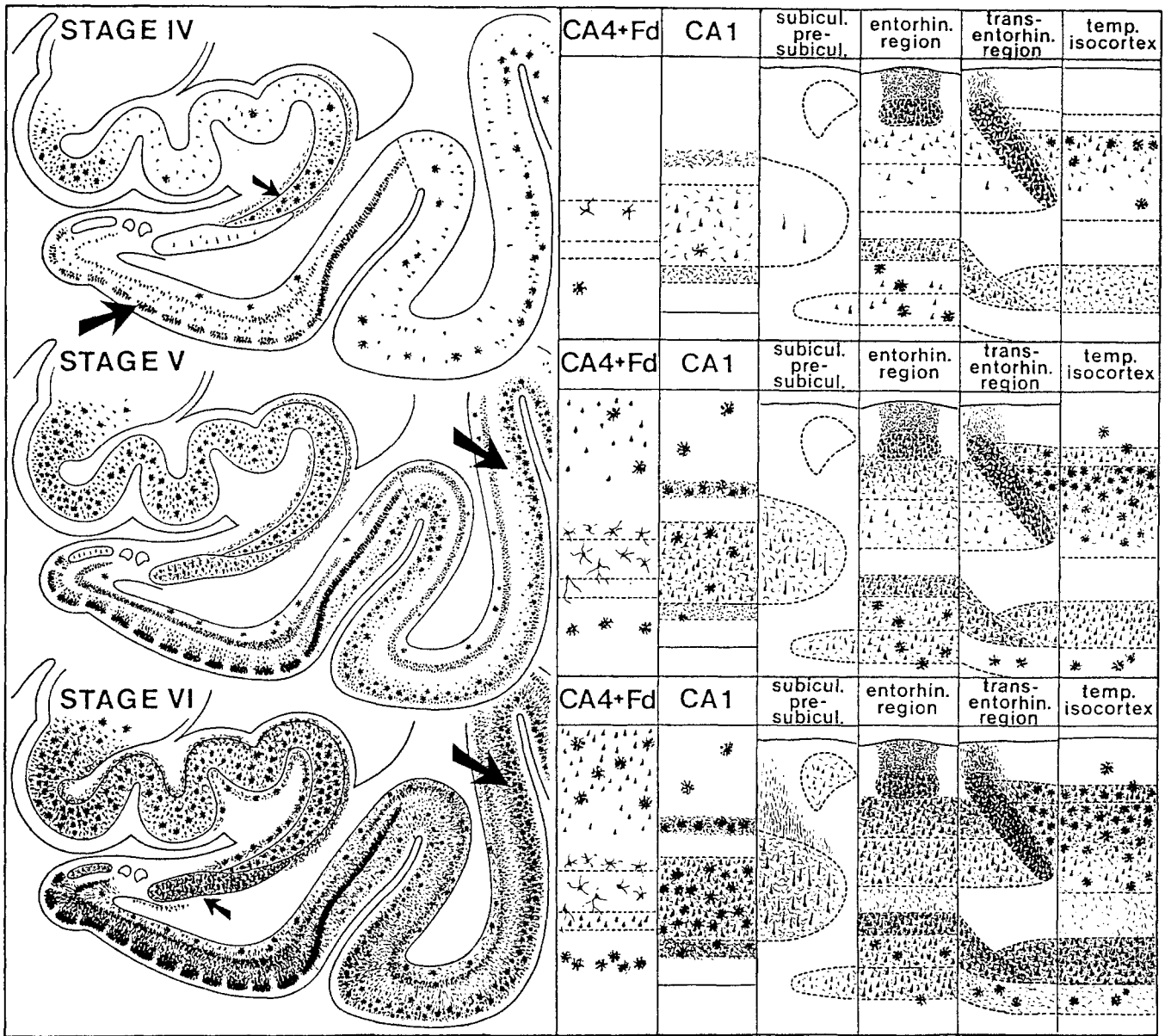
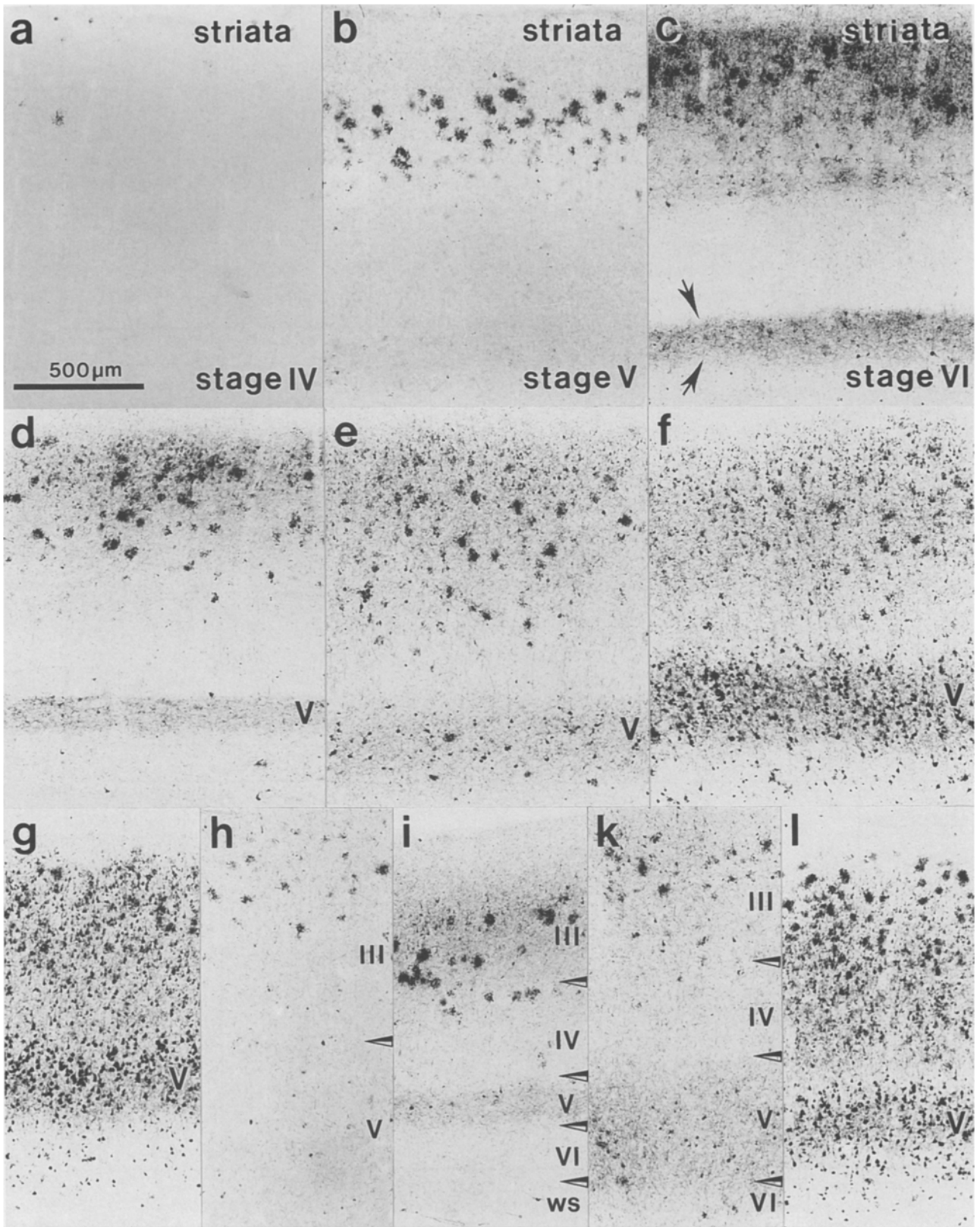
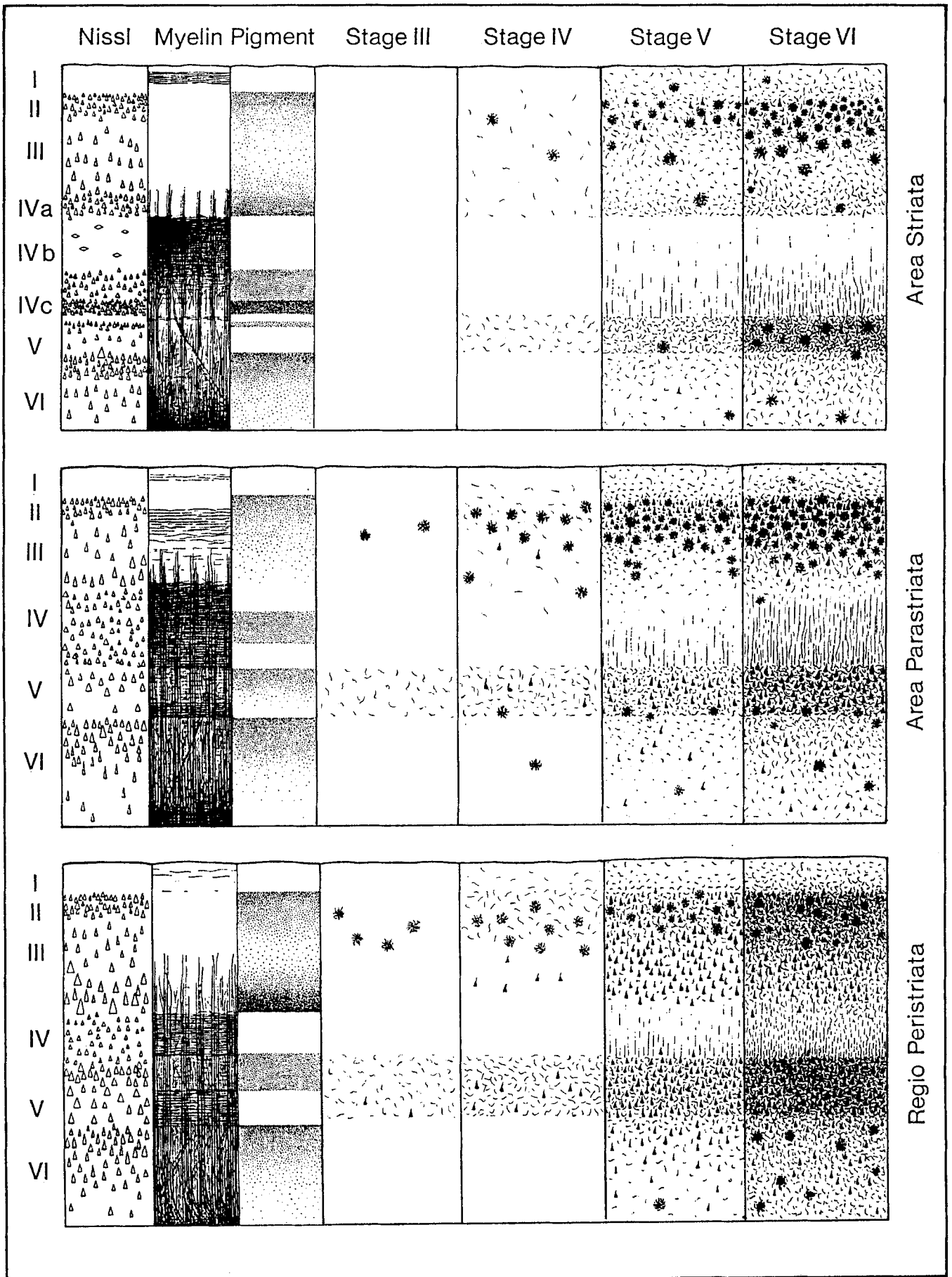


Fig. 10.

**Figs. 9, 10.** Summary diagrams of cortical NF changes seen in stages I–VI of Alzheimer’s disease. Mild and severe destruction of the transentorhinal layer Pre- $\alpha$  characterizes the transentorhinal stages I and II. The two forms of limbic stages (III and IV) are marked by conspicuous involvement of layer Pre- $\alpha$  in both the transentorhinal region and proper entorhinal region. The hallmark of the two forms of isocortical stages (V and VI) is a severe destruction of isocortical association areas. The large arrows point to the leading characteristics, smaller ones indicate additional features. Areas and layers are outlined in stage I. *a*: alveus; *CA1*: first sector of the Ammon’s horn; *CA4*: fourth sector of the Ammon’s horn; *Diss*: lamina dissecans; *entorhin.*: entorhinal; *Fd*: fascia dentata; *gr*: granule cell layer of the fascia dentata; *m*: molecular layer of sector CA1; *mo*: molecular layer of the fascia dentata; *o*: stratum oriens; *p*: pyramidal cell layers of sector CA1; *parasubic*: parasubiculum; *pl*: plexiform layer of the fascia dentata; *pr*: parvocellular layer of the presubiculum; *Pre- $\alpha, \beta, \gamma$* : lamina principalis externa, layer  $\alpha, \beta, \gamma$ ; *Pri- $\alpha, \beta, \gamma$* : lamina principalis interna, layer  $\alpha, \beta, \gamma$ ; *presubic*: presubiculum proper; *sub*: subiculum; *temp.*: temporal; *transentorhin.*: transentorhinal; *I–VI*: isocortical layers

**Fig. 11a–l.** Isocortical NF changes. **a** The striate area is virtually devoid of NF changes or shows only a few isolated NP in stage IV (case no. 59). **b** The same field exhibits mainly NP in layer III in stage V (case no. 68). **c** Layer III involvement is aggravated in stage VI (case no. 72). A few NFT-bearing nerve cells can at this stage also be seen. The hallmark of stage VI, however, is a dense network of NT in layer V of the striate area indicated by arrows. **d–l** Isocortical involvement in stage VI (case no. 79). **d** striate area (core); **e** parastriate field (belt); **f** peristriate region (association areas). Note the increasing involvement of layer V as one proceeds from the primary area through the belt field to the association cortex. **g** Frontal association cortex; **h** somato-motor core field (posterior bank of precentral gyrus); **i** somato-sensory core field (anterior bank of postcentral gyrus); **k** auditory core field (proximal half of Heschl’s gyrus). Note the presence of NP in layer III of primary fields. A dense network of NT is developed in layer V of only the sensory core fields. **l** Temporal association cortex. Note the abundance of NP in layer III. The scale in **a** is also valid for **b–l**. *I–VI*: isocortical layers. **WS**: white substance. PEG sections, 100  $\mu$ m, Gallyas





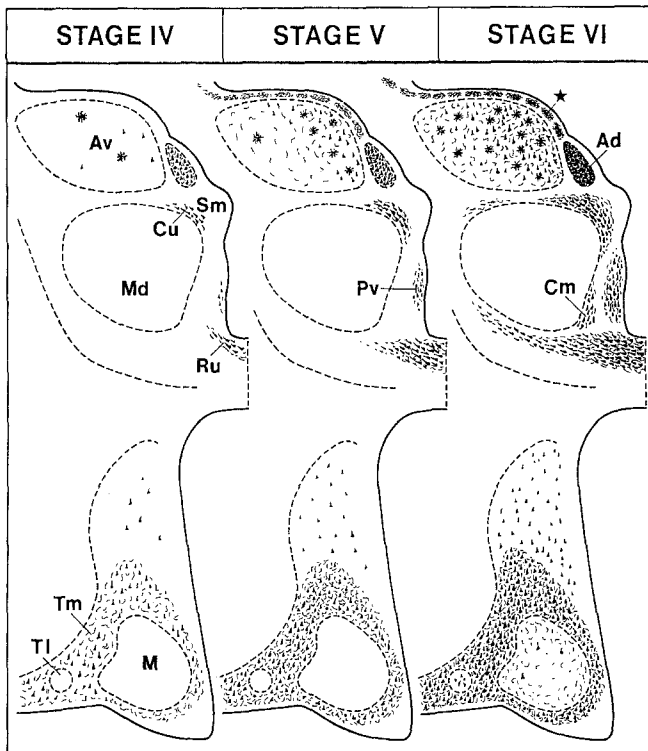


**Fig. 13.** Summary diagram of NF changes in both the thalamus and hypothalamus. *Ad*: Antero-dorsal nucleus; *Av*: antero-ventral nucleus; *Cm*: central medial nucleus; *Cu*: cucullar nucleus (part of the central medial nucleus); *M*: mamillary body; *Md*: medio-dorsal nucleus; *Pv*: paraventricular nucleus of the thalamus; *Ru*: reuniens nucleus; *Sm*: stria medullaris; *TI*: lateral tuberal nucleus, *Tm*: tuberomamillary nucleus; *asterisks*: dense network of argyrophilic processes located between the antero-ventral nucleus and the ependymal lining of the third ventricle

to the soma and differ considerably from the star-shaped NFT present in the plexiform layer of the fascia dentata (Fig. 8c–d). Even the granule cells of the fascia dentata may show a few dot-like NFT (Fig. 8a,b, and second row).

The main feature of stage V, however, is that the isocortex is severely affected. In cases in which the isocortex is only mildly affected, changes are confined to the retrosplenial region, the basal portions of the medial facies and the entire inferior facies of both the temporal and the occipital lobe. Antero-basal portions of the insula and orbitofrontal cortex follow. In cases in which the isocortex is more severely affected, these areas tend to show the highest packing density of NFT and NT (Fig. 4). The temporal isocortex – with the exception of the

first temporal gyrus – is characterized by a particularly large number of NP in layer III (Fig. 11i). Virtually all isocortical association areas are affected. The material examined does not permit distinction of “anterior” or “posterior” types, i.e., predominance of the changes in frontal or parietal-occipital-temporal association areas (Fig. 4). Primary sensory areas are still more or less resistant to the development of pathological changes showing only modest numbers of NP in layer III (Fig. 11b) with layer V being only initially affected. The primary motor field shows sparse numbers of NP in layer III and is the last component of the isocortex affected by the pathological process.

The subcortical nuclei mentioned in stage IV show a much more pronounced alteration. Basal portions of the claustrum abutting upon the amygdala are now consistently involved. The antero-dorsal nucleus of the thalamus reveals considerable loss of nerve cells and presence of numerous ghost tangles. The antero-ventral nucleus displays initial NF changes (Fig. 13). Another new component appearing in stage V is a brushwork of argyrophilic cellular processes covering the antero-ventral nucleus [10]. A few NFT and NT can also be observed in the lateral tuberal nucleus of the hypothalamus and in pars compacta of the substantia nigra.

*Stage VI.* In stage VI all these changes are even more pronounced. Considerable loss of nerve cells is seen in layers Pre- $\alpha$  and Pri- $\alpha$  and is paralleled by large numbers of ghost tangles (Fig. 6d). Occasionally, even the ghost tangles have been degraded and replaced by glial cell accumulations. The parvocellular layers of the parasubiculum and transsubiculum contain many small NFT and develop a dense web of NT.

The hippocampal formation is infested with NF changes (Fig. 8). The large number of NFT-bearing granule cells in the fascia dentata facilitates differentiation of stage V from stage VI (Fig. 8, second row). CA1 is characterized by severe loss of nerve cells, presence of numerous ghost tangles and clear-cut stripes of NT within the upper half of the stratum radiatum and within the stratum oriens (Fig. 8, third row). The subiculum still exhibits an only modest number of NFT but is densely filled with NT (Fig. 8, fourth row, and Fig. 10, third row).

All isocortical association areas are very severely affected. A special feature of primary sensory areas is the presence of a dense network of NT contrasted by only small numbers of NFT in layer V which thus appears as a darkly stained band with clear cut boundaries (Figs. 11c,d,i,k, 12). This pattern can readily be recognized in the narrow fifth layer of the striate area and represents a further difference between stage V and stage VI (Fig. 11c,d). The primary motor field, in contrast, does not develop a comparable alteration of layer V. With the exception of some layer III NP it remains almost devoid of NF changes (Fig. 11h).

Involvement of subcortical nuclei is very severe and does not contribute much to the differentiation of stages. The network of pathologically changed cellular processes covering the antero-ventral nucleus now

**Fig. 12.** Summary diagram of NF changes seen in the occipital isocortex in stages III–VI. At the left-hand border a synopsis of the cyto-, myelo-, and pigmentoarchitectonic scheme is given of the striate area (core field), the parastriate field (belt area), and the peristriate region (association cortex). NP and NT predominate in the core field while NFT can mainly be seen in the association cortex

extends into the reticular nucleus of the thalamus (Fig. 13, asterisk). Antero-dorsal portions of this nucleus appear to be particularly affected. The severity of the change gradually decreases when approaching the lateral and postero-ventral extremities of the nucleus [10, 57]. NFT-bearing neurons can be encountered in the lateral tuberal nucleus of the hypothalamus.

Stage VI is, furthermore, characterized by the involvement of the extrapyramidal system. Most of the large and quite a number of the medium-sized nerve cells of the striatum contain a NFT [7]. In addition, NFT with far-reaching dendritic extensions can be observed in many of the melanin-containing neurons of the substantia nigra.

The obvious hallmark of stages V and VI is that the isocortex is devastatingly affected. The pathology includes, of course, all the changes noted in earlier stages (Figs. 4, 12). Stages V and VI are, therefore, denoted as "isocortical stages".

## Discussion

Insidious onset and continual progress of dementia in a state of clear consciousness characterize AD [37, 42, 54]. The speed of mental deterioration is subject to inter-individual variation. This explains the existence of marked differences in the duration of the disease. The clinical course can be subdivided into a number of stages for better recognition and control of the progress of the disease [29, 36, 45–47, 50].

Individuals suffering from AD develop pathological changes of the brain. Most conspicuous is the occurrence of extracellular amyloid and intraneuronal NF changes. Accumulation of this pathological material commences before the appearance of clinical symptoms (preclinical phase).

### *Amyloid deposits*

Depositions of amyloid are among the first changes seen in the brain. Most of them do not correspond to NP [15]. Size and shape of the deposits and their distribution pattern vary from one individual to another. Characteristics of amyloid deposits, therefore, are of limited significance for differentiation of stages.

The fact that accumulations of amyloid are frequently found in the cortex of non-demented individuals in the absence of NF changes ([21]; cases nos. 1–3, 7, 10, 11) has led to the assumption that depositions of amyloid precede the development of NF changes [22, 27]. It is, therefore, important to note that in quite a number of cases one can also recognize a contrasting pattern with cortical NF changes preceding the deposition of amyloid (Table 2, nos. 12, 13, 21, 22, 25, 26, 29, 30, 36, 37, 41, 50). The existence of amyloid deposits can, thus, not be considered as a prerequisite for the development of NF changes [52]. It remains to be elucidated whether there is a relationship at all between amyloid and NF changes.

### *Neurofibrillary changes*

Intraneuronal NF changes can be observed in NP, NFT and NT. The distribution pattern of NP is different from that of NFT and NT. In general, the occurrence of NFT and NT precedes that of NP. NP frequently show a patchy distribution with varying densities even within the boundaries of architectonic units [14, 18, 49, 59]. Moreover, their distribution pattern is subject to considerable inter-individual variation. The inconsistent presence, density and distribution pattern of NP, therefore, prevents neuropathological staging [23].

NFT and NT, in contrast, exhibit a well-defined pattern [20, 30, 34, 60], permitting differentiation of stages. They ultimately lead to the destruction of many of the affected nerve cells which is documented by the appearance of "ghost" tangles in many cortical areas and subcortical nuclei [1]. Considerable loss of nerve cells confined to circumscribed areas of gray matter will almost certainly cause functional deficits contributing to the clinical symptoms of AD.

Given the existence of a preclinical phase of AD one would expect to find a small amount of NF changes in a number of non-demented individuals, while demented patients should show comparable changes in higher density. The material examined can, in fact, be arranged in such a manner as to form a row with gradually increasing density of NFT and NT (Tables 1, 2).

For practical purposes one should initially classify a case as belonging to either the "transentorhinal", the "limbic", or the "isocortical" stages and, thereafter, decide whether it is a mild or severe version of the respective stages.

The transentorhinal stages most probably represent clinically silent periods of the disease (preclinical phase, Table 2). They can easily be overlooked when using the conventional hippocampus preparation cut out at the level of the lateral geniculate body. This is because both the entorhinal and transentorhinal region are either missing at this level or present with only remnants of their posterior poles (Fig. 14). The hippocampus preparation, therefore, does not allow recognition of transentorhinal stages. It also does not permit diagnosis of an unaffected cortex (a false diagnosis caused by absence of NF changes in both the hippocampus and the temporal isocortex). A prerequisite for detection of transentorhinal stages is, thus, an additional section cut out at the level of the uncus (Figs. 7, 9, 10, 14). The particular advantage of this "entorhinal" preparation is the clear demonstration of the wedge-shaped extremity of CA1 (prosubiculum), the wing-shaped profile of the subiculum, the presubiculum, parasubiculum, entorhinal region, transentorhinal region and adjoining temporal isocortex (Figs. 7, 9, 10).

It appears possible that the limbic stages correspond to clinically incipient AD ([9]; Table 2). The limbic stages are characterized by the entorhinal region being severely affected with a moderate involvement of the first Ammon's horn sector. The CA1 is initially affected in the wedge-shaped extremity superimposing on the subiculum and extends from hereon towards CA2. Involvement

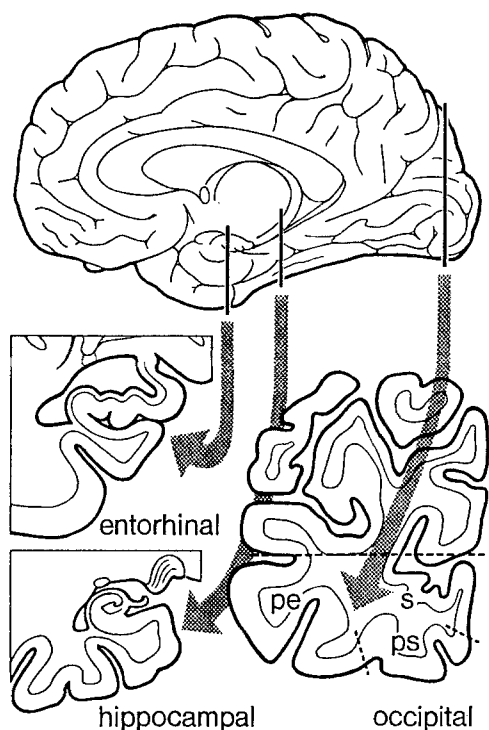


**Fig. 14.** Scheme of the three preparations which are prerequisites for neuropathological staging of Alzheimer-related NF changes. The first preparation runs through the uncus and displays the entorhinal and transentorhinal region. The second block is cut out at the level of the lateral geniculate body and provides the conventional view of the hippocampal formation. The third preparation runs through the occipital pole and includes (*s*) the striate area, (*ps*) the parastriate field, and (*pe*) the peristriate region

ment of CA2 is subject to considerable inter-individual variation and is, therefore, intentionally not included as a diagnostic criterion. The isocortex in the limbic stages should either be devoid of NF changes or should only exhibit a mild affection (Figs. 7, 9, 10). A section running through the occipital pole is recommended (isocortical preparation) containing a primary sensory field (striate area) with clear-cut borderlines, a belt area (parastriate field) and, in addition, association cortex (peristriate region; Fig. 14). Severe alteration of the peristriate cortex is incompatible with the diagnosis of limbic stages.

The isocortical stages ultimately correspond to fully developed AD (the clinical protocols of all isocortical stages note the presence of dementia; Table 2). The isocortical preparation showing the striate area, the parastriate field and the peristriate region is well suited for differentiation of stage V from stage VI. The primary sensory areas generally are less severely affected than the association areas [24, 44] and it is only in stage VI that a wealth of NT in layer V can be seen (Figs. 11c,d,i,k; 12). This pattern is clearly observable in the postcentral somatosensory core field and the primary acoustic area (Fig. 11i,k), but for practical purposes it appears much more convenient to check NT density in layer V of the striate area (Figs. 11c,d; 12). Preparations

showing nuclei of the thalamus, hypothalamus and lower brain stem also reveal a sequence of involvement (Fig. 13, Table 1) which appears to be a trifle less consistent when compared to the changes seen in the cerebral cortex.

After application of the conventional diagnostic criteria [23, 32, 35, 61], only the most severe cases of AD can be set off from a broad spectrum of cases with different degrees of dementia. It appears unsatisfying to classify the latter as “non-AD” cases. In fact, AD is a gradually progressing process which does not allow one to draw such a sharp borderline. The distinction of stages appears to be far more appropriate. The present study shows that stage differentiation can be based upon qualitative evaluation of changes in the distribution pattern of NFT and NT (Tables 1, 2). Recognition of the six stages under consideration requires a minimum of three sections (Fig. 14; hippocampal, entorhinal and occipital isocortical preparation) and does not include quantitative evaluations. Speed and simplicity are the particular advantages of the proposed procedure.

*Acknowledgements.* The authors are indebted to Professors Hübner, Stutte, Schlote, Goebel and Bohl (Departments of Pathology and Neuropathology, Frankfurt and Mainz) for providing the autopsy material. The antibodies were generously provided by Professors Beyreuther (Heidelberg; anti-A4), Grundke-Iqbal and Iqbal (Staten Islands, New York; anti PHF). The skilful technical assistance of Ms Babl, Fertig, Schneider (preparations), Szasz (drawings), and Mr. Müller (secretarial help) is gratefully acknowledged.

## References

- Bondareff W, Mountjoy CQ, Roth M, Hauser DL (1989) Neurofibrillary degeneration and neuronal loss in Alzheimer's disease. *Neurobiol Aging* 10:709–715
- Braak H (1980) Architectonics of the human telecephalic cortex. In: Braitenberg V, Barlow HB, Bizzi E, Florey E, Grüsser OJ, van der Loos H (eds) *Studies of brain function*, vol 4. Springer, Berlin Heidelberg New York, pp 1–147
- Braak H, Braak E (1985) On areas of transition between entorhinal allocortex and temporal isocortex in the human brain. Normal morphology and lamina-specific pathology in Alzheimer's disease. *Acta Neuropathol (Berl)* 68:325–332
- Braak H, Braak E (1988) Morphology of the human isocortex in young and aged individuals: qualitative and quantitative findings. *Interdiscip Top Gerontol* 25:1–15
- Braak H, Braak E (1988) Neurofil threads occur in dendrites of tangle-bearing nerve cells. *Neuropathol Appl Neurobiol* 14:39–44
- Braak H, Braak E (1989) Cortical and subcortical argyrophilic grains characterize a disease associated with adult onset dementia. *Neuropathol Appl Neurobiol* 15:13–26
- Braak H, Braak E (1990) Alzheimer's disease: striatal amyloid deposits and neurofibrillary changes. *J Neuropathol Exp Neurol* 49:215–224
- Braak H, Braak E (1990) Morphology of the cerebral cortex in relation to Alzheimer's dementia. In: Maurer K, Riederer P, Beckmann H (eds) *Alzheimer's disease. Epidemiology, Neuropathology, Neurochemistry, and Clinics. Key Topics in Brain Research*. Springer Wien, pp 85–91

9. Braak H, Braak E (1990) Neurofibrillary changes confined to the entorhinal region and an abundance of cortical amyloid in cases of presenile and senile dementia. *Acta Neuropathol* 80:479–486
10. Braak H, Braak E (1991) Alzheimer's disease affects limbic nuclei of the thalamus. *Acta Neuropathol* 81:261–268
11. Braak H, Braak E (1991) Demonstration of amyloid deposits and neurofibrillary changes in whole brain sections. *Brain Pathol* 1:213–216
12. Braak H, Braak E, Grundke-Iqbal I, Iqbal K (1986) Occurrence of neuropil threads in the senile human brain and in Alzheimer's disease: a third location of paired helical filaments outside of neurofibrillary tangles and neuritic plaques. *Neurosci Lett* 65:351–355
13. Braak H, Braak E, Ohm T, Bohl J (1988) Silver impregnation of Alzheimer's neurofibrillary changes counterstained for basophilic material and lipofuscin pigment. *Stain Technol* 63:197–200
14. Braak H, Braak E, Kalus P (1989) Alzheimer's disease: areal and laminar pathology in the occipital isocortex. *Acta Neuropathol* 77:494–506
15. Braak H, Braak E, Ohm T, Bohl J (1989) Alzheimer's disease: mismatch between amyloid plaques and neuritic plaques. *Neurosci Lett* 103:24–28
16. Braak H, Braak E, Bohl J, Lang W (1989) Alzheimer's disease: amyloid plaques in the cerebellum. *J Neurol Sci* 93:277–287
17. Campbell SK, Switzer RC, Martin TL (1987) Alzheimer's plaques and tangles: a controlled and enhanced silver-staining method. *Soc Neurosci Abstr* 13:678
18. Castano EM, Frangione B (1988) Biology of disease. Human amyloidosis, Alzheimer's disease and related disorders. *Lab Invest* 58:122–132
19. Davies L, Wolska B, Hilbich C, Multhaup G, Martins R, Simms G, Beyreuther K, Masters CL (1988) A4 amyloid protein deposition and the diagnosis of Alzheimer's disease: prevalence in aged brains determined by immunocytochemistry compared with conventional neuropathologic techniques. *Neurology* 38:1688–1693
20. Dayan AD (1970) Quantitative histological studies on the aged human brain. I. Senile plaques and neurofibrillary tangles in normal patients. *Acta Neuropathol (Berl)* 16:85–94
21. Delaère P, Duyckaerts C, Masters C, Beyreuther K, Piette F, Hauw JJ (1990) Large amounts of neocortical  $\beta$ A4 deposits without neuritic plaques nor tangles in a psychometrically assessed, non-demented person. *Neurosci Lett* 116:87–93
22. Duyckaerts C, Delaère P, Poulain V, Brion JP, Hauw JJ (1988) Does amyloid precede paired helical filaments in the senile plaques? A study of 15 cases with graded intellectual status in aging and Alzheimer's disease. *Neurosci Lett* 91:354–359
23. Duyckaerts C, Delaère P, Hauw JJ, Abbamondi-Pinto AL, Sorbi S, Allen I, Brion JP, Flament-Durand J, Duchon L, Kauss J, Schlote W, Lowe J, Probst A, Ravid R, Swaab DF, Renkawek K, Tomlinson B (1990) Rating of lesions in senile dementia of the Alzheimer type: concordance between laboratories. A European multicenter study under the auspices of EURAGE. *J Neurol Sci* 97:295–323
24. Esiri MM, Pearson RCA, Powell TPS (1986) The cortex of the primary auditory area in Alzheimer's disease. *Brain Res* 366:385–388
25. Gallyas F (1971) Silver staining of Alzheimer's neurofibrillary changes by means of physical development. *Acta Morphol Acad Sci Hung* 19:1–8
26. Gallyas F, Wolff JR (1986) Metal-catalyzed oxidation renders silver intensification selective. Applications for the histochemistry of diaminobenzidine and neurofibrillary changes. *J Histochem Cytochem* 34:1667–1672
27. Giaccone G, Tagliavini F, Linoli G, Bouras C, Frigero B, Bugiani O (1989) Down patients: extracellular preamyloid deposits precede neuritic degeneration and senile plaques. *Neurosci Lett* 97:232–238
28. Grünthal E (1930) Die pathologische Anatomie der senilen Demenz und der Alzheimerschen Krankheit. In: Bumke O (ed) *Handbuch der Geisteskrankheiten. Die Anatomie der Psychosen*, vol 11. Springer, Berlin, pp 638–672
29. Gutzmann H (1988) *Senile Demenz vom Alzheimer Typ*. Enke, Stuttgart, pp 1–130
30. Hubbard BM, Fenton GW, Anderson JM (1990) A quantitative histological study of early clinical and preclinical Alzheimer's disease. *Neuropathol Appl Neurobiol* 16:111–121
31. Hyman BT, van Hoesen GW, Damasio AR, Barnes CL (1984) Alzheimer's disease: cell-specific pathology isolates the hippocampal formation. *Science* 25:1168–1170
32. Jellinger K, Lassmann H, Fischer P, Danielczyk W (1991) Validation of diagnostic criteria for Alzheimer's disease. In: Iqbal K, McLachlan DRC, Winblad B, Wisniewski HM (eds) *Alzheimer's disease: basic mechanisms, diagnosis and therapeutic strategies*, Wiley, Chichester, pp 75–89
33. Kalus P, Braak H, Braak E, Bohl J (1989) The presubicular region in Alzheimer's disease: topography of amyloid deposits and neurofibrillary changes. *Brain Res* 494:198–203
34. Kemper TL (1978) Senile dementia: a focal disease in the temporal lobe. In: Nandy E (ed) *Senile dementia: a biomedical approach*. Elsevier, Amsterdam, pp 105–113
35. Khachaturian ZS (1985) *Diagnosis of Alzheimer's disease*. *Arch Neurol* 42:1097–1105
36. Kurz AF, Lauter H, Zimmer R (1988) What are the early and late clinical manifestations of the disease? In: Henderson AS, Henderson JH (eds) *Etiology of dementia of Alzheimer's type*. Wiley and Sons, Chichester New York Brisbane Toronto Singapore, pp 83–103
37. Lauter H, Kurz A, Haupt M, Romero B, Zimmer R (1990) Clinical diagnosis of Alzheimer's disease: DSM-III-R, ICD-10 – what else? In: Maurer K, Riederer P, Beckmann H (eds) *Alzheimer's disease. Epidemiology, Neuropathology, Neurochemistry, and Clinics. Key Topics in Brain Research*. Springer, Wien, pp 365–371
38. Lewis DA, Campbell MJ, Terry RD, Morrison JH (1987) Laminar and regional distributions of neurofibrillary tangles and neuritic plaques in Alzheimer's disease: a quantitative study of visual and auditory cortices. *J Neurosci* 7:1799–1808
39. Mann DMA (1985) The neuropathology of Alzheimer's disease: a review with pathogenetic, aetiological and therapeutic considerations. *Mech Ageing Dev* 31:213–255
40. Mann DMA, Jones D, Prinja D, Purkiss MS (1990) The prevalence of amyloid (A4) protein deposits within the cerebral and cerebellar cortex in Down's syndrome and Alzheimer's disease. *Acta Neuropathol* 80:318–327
41. Masliah E, Terry RD, Mallory M, Alford M, Hansen LA (1990) Diffuse plaques do not accentuate synapse loss in Alzheimer's disease. *Am J Pathol* 137:1293–1297
42. McKhann G, Drachman D, Folstein MF, Katzman R, Price D, Stadlan EM (1984) Clinical diagnosis of Alzheimer's disease: report of the NINCDS-ADRDA-work group under the auspices of department of health and human services, task force on Alzheimer's disease. *Neurology* 34:939–944
43. Ogomori K, Kitamoto T, Tateishi J, Sato Y, Suetsugu M, Abe M (1989)  $\beta$ -Protein amyloid is widely distributed in the central nervous system of patients with Alzheimer's disease. *Am J Pathol* 134:243–251
44. Pearson RCA, Esiri MM, Hiorns W, Wilcock GK, Powell TPS (1985) Anatomical correlates of the distribution of the pathological changes in the neocortex in Alzheimer's disease. *Proc Natl Acad Sci USA* 82:4531–4534
45. Reisberg B, Ferris SH, Anand R, DeLeon MJ, Schneck MK, Buttinger C, Borenstein J (1984) Functional staging of dementia of the Alzheimer type. *Ann NY Acad Sci* 435:481–483
46. Reisberg B, Ferris SH, DeLeon MJ (1985) Senile dementia of the Alzheimer type: diagnostic and differential diagnostic features with special reference to functional assessment stag-

- ing (FAST). In: Traber J, Gispén WH (eds) *Senile dementia of the Alzheimer Type*. Springer, Berlin Heidelberg New York Tokio, pp 18–37
47. Reisberg B, Ferris SH, DeLeon MJ, Kluger A, Franssen E, Borenstein J, Alba RC (1989) The stage specific temporal course of Alzheimer's disease: functional and behavioral concomitants based upon cross-sectional and longitudinal observation. In: Iqbal K, Wisniewski HM, Winblad B (eds) *Alzheimer's disease and related disorders*. Liss, New York, pp 23–41
  48. Rogers J, Morrison JH (1985) Quantitative morphology and regional and laminar distributions of senile plaques in Alzheimer's disease. *J Neurosci* 5:2801–2808
  49. Simchowicz T (1911) *Histologische Studien über die senile Demenz*. In: Nissl F, Alzheimer A (eds) *Histologische und histopathologische Arbeiten über die Großhirnrinde mit besonderer Berücksichtigung der pathologischen Anatomie der Geisteskrankheiten*, vol 4. Fischer, Jena, pp 267–444
  50. Sjögren T, Sjögren H, Lindgren AGH (1952) *Morbus Alzheimer and Morbus Pick*. *Acta Psychiatr Neurol Scand [Suppl]* 82:1–152
  51. Smithson KG, MacVicar BA, Hatton GI (1983) Polyethylene glycol embedding: a technique compatible with immunocytochemistry, enzyme histochemistry, histofluorescence and intracellular staining. *J Neurosci Methods* 7:27–41
  52. Tabaton M, Mandybur TI, Perry G, Onorato M, Autilio-Gambetti L, Gambetti P (1989) The widespread alteration of neurites in Alzheimer's disease may be unrelated to amyloid deposition. *Ann Neurol* 26:771–778
  53. Terry RD (1985) Alzheimer's disease. In: Davis RL, Robertson DM (eds) *Textbook of neuropathology*. Williams and Wilkins, Baltimore, pp 824–841
  54. Tierney MC, Fisher RH, Lewis AJ, Zorzitto ML, Snow WG, Reid DW, Nieuwstaten P (1988) The NINCDS-ADRDA work group criteria for the clinical diagnosis of probable Alzheimer's disease: a clinicopathologic study of 57 cases. *Neurology* 38:359–364
  55. Tomlinson BE (1989) The neuropathology of Alzheimer's disease – Issues in need of resolution. *Neuropathol Appl Neurobiol* 15:491–512
  56. Tomlinson BE, Corsellis JAN (1984) Ageing and the dementias. In: Adams JH, Corsellis JAN, Duchon LW (eds) *Greenfield's neuropathology*. Arnold, London, pp 951–1025
  57. Tourtellotte WG, van Hoesen GW, Hyman BT, Tikoo RK, Damasio AR (1989) Alz-50 immunoreactivity in the thalamic reticular nucleus in Alzheimer's disease. *Brain Res* 515:227–234
  58. Van Hoesen GW, Hyman BT (1990) Hippocampal formation: anatomy and the patterns of pathology in Alzheimer's disease. *Prog Brain Res* 83:445–457
  59. Von Braunmühl A (1957) *Alterserkrankungen des Zentralnervensystems. Senile Involution. Senile Demenz. Alzheimersche Krankheit*. In: Lubarsch O, Henke F, Rössle R (eds) *Handbuch der speziellen pathologischen Anatomie und Histologie*, vol 13/1A. Springer, Berlin, pp 337–539
  60. Wilcock G, Esiri MM (1982) Plaques, tangles and dementia. A quantitative study. *J Neurol Sci* 56:343–356
  61. Wisniewski HM, Rabe A, Zigman W, Silverman W (1989) Neuropathological diagnosis of Alzheimer's disease. *J Neuropathol Exp Neurol* 48:606–609
  62. Yamaguchi H, Hirai S, Morimatsu M, Shoji M, Ihara Y (1988) A variety of cerebral amyloid deposits in the brains of the Alzheimer-type dementia demonstrated by  $\beta$  protein immunostaining. *Acta Neuropathol* 76:541–549
  63. Yamaguchi H, Nakazato Y, Shoji M, Ihara Y, Hirai S (1990) Ultrastructure of neuropil threads in the Alzheimer brain: their dendritic origin and accumulation in the senile plaques. *Acta Neuropathol* 80:368–374